Journal of Hazardous Materials 171 (2009) 93–101

Contents lists available at ScienceDirect

Journal of Hazardous Materials

journal homepage: www.elsevier.com/locate/jhazmat

Elaboration, characterization and application of polysulfone and polyacrylic acid blends as ultrafiltration membranes for removal of some heavy metals from water

Chamekh Mbareck[a,*], Quang Trong Nguyen[b], Ouafa Tahiri Alaoui[b], Daniel Barillier[c]

[a] Université de Nouakchott, Faculté des Sciences et Techniques, B.P. 5026, Nouakchott, Mauritania
[b] P.B.S. Université de Rouen, 76821 Mont-Saint-Aignan, France
[c] ERPCB, EA3914, IUT-UFR Sciences, Université de Caen, 14032 Caen Cedex, France

ARTICLE INFO

Article history:
Received 4 October 2008
Received in revised form 7 May 2009
Accepted 25 May 2009
Available online 6 June 2009

Keywords:
Polymer blends
Ultrafiltration membrane
Water depollution
Lead
Heavy metal
SEM-EDX

ABSTRACT

Polysulfone (PSf)/polyacrylic acid ultrafiltration (PSf/PAA) membranes were prepared from a polymer blend in dimethylformamide by coagulation in water according to the wet phase inversion method. Immobilization of water-soluble PAA within the non-soluble PSf matrix was proven by the increase of ion exchange capacity and the intensity of the carboxyl groups' peak with the increase of PAA content as shown by Fourier transform infrared spectra. These results lead to consider that PSf and PAA form a semi-interpenetrating polymer networks. The obtained membranes showed a decrease of mean surface-pore sizes, the overall porosity and the hydraulic permeability with the increase in PAA content. Such results were imputed to the morphologic modifications of PSf film with the immobilization of increasing PAA amount.

PSf/PAA membranes showed high lead, cadmium and chromium rejection which reaches 100% at pH superior to 5.7 and a low rejection at low pH. Moreover, the heavy metal rejection decreases with feed solution concentration and applied pressure increases. These behaviors were attributed to the role of carboxylic groups in ion exchange or complexation. As a matter of fact, the strong lead ion–PAA interactions were revealed by the scanning electron microscopy with energy dispersive X-rays (SEM-EDX).

1. Introduction

Membrane processes are increasingly used in the environment protection, drinking-water production and medical applications [1–3]. These processes are widely used in many countries (Gulf countries, Japan) to produce drinking water, to recover reusable components or to purify industrial effluents, etc. Pollution of water sources is usually due to human activities that lead to the presence of toxic species like pesticides, microorganisms, dyes and heavy metals in surface water, and eventually in ground water. Heavy metals are well known for their high toxicity for human beings. They are soluble in water as ions or chemical complexes and they could be ingested if water is not correctly treated [4–8]. Various techniques have been devoted to the removal of these metals from water [9–11]. Over the last few years, several works were dedicated to the purification of water and effluents, containing heavy metal, with ultrafiltration assisted by complexation [12–15]. The complexing agents were added to the feed water to form high molecular-weight complexes with heavy metal ions. Such complexation prevents the heavy metal ion permeation through ultra/nanofiltration membranes.

Polyelectrolytes like polyacrylic acid (PAA), polystyrene sodium sulfonate (PSSNa) and polyethylenimine (PEI) [16–26] were used as complexing agents for the removal of heavy metal ions from water. These additives are generally pre-mixed with water before treatment by ultrafiltration in order to permit the complexation of heavy metal ions at an appropriate pH. However, in such a technique, there is a risk of more severe fouling due to the lower diffusivity of the large-size complexed species, and their lower hydrophilicity after charge coupling in the complexes [27]. In addition, alternative membrane-based processes were achieved by incorporation of ionic groups in preformed-membrane surface [28–30].

In water filtration processes, incorporation of charges in the membrane is expected to reduce considerably the fouling effect, improve membrane efficiency and increase the membrane life. The main methods used to impart charges to polysulfone membranes were (i) sulfonation: insertion of sulfonate groups, (ii) carboxylation: insertion of carboxylic acid groups and (iii) quaternization: insertion of quaternary ammonium groups [31–34]. However, it can be predicted from the general polymer chemistry knowledge that the polysulfone chains undergo upon chemical modifications chain

* Corresponding author.
E-mail address: chamec1@yahoo.fr (C. Mbareck).

0304-3894/$ – see front matter © 2009 Elsevier B.V. All rights reserved.
doi:10.1016/j.jhazmat.2009.05.123

degradation, surface smoothness alteration and sometimes become highly swollen, leading to a decrease in the membrane mechanical properties.

Due to its simplicity, polymer blending is an attractive technique for the design of new materials [35,36]. However, its use is limited by the lack of polymer systems in which the polymer components are enough miscible for the target applications. In a previous paper [37], we described for the first time, preparation of ultrafiltration membranes by blending poly(acrylic acid) with uncharged polysulfone. Polymers formed a chemical structure reminiscent of semi-interpenetrating polymer networks, with an asymmetric morphology. The formation of this network was interpreted as a result of hydrophobic interactions between polysulfone chains during the coagulation process.

The present paper aims at exploring the membrane performances in the removal of heavy metal ions from water. Prior to the attempt of metal-ion removal, the membranes were characterized by different techniques. Membrane morphology, porosity, swelling ratio, and polyelectrolyte entrapment were studied by using scanning electron microscopy (SEM), electron dispersive X-rays (EDX) and Fourier transform infrared (FTIR). The influence of metal-ion concentration and pH of the feed solution, and of the transmembrane pressure on the heavy metal retention has been analyzed by atomic absorption spectroscopy, AAS.

2. Experimental

2.1. Materials

Polysulfone (PSf) and polyacrylic acid (PAA) were purchased from Aldrich and dimethylformamide (DMF) from VWR (Fontenay sous Bois, France). The molecular weights of PAA and PSf were 450,000 and 26,000 g/mol, respectively. Poly(ethylene glycol) was purchased from Sigma–Aldrich. All polymers and chemical products were used as received.

2.2. Membrane preparation and morphological characterization

Polysulfone (PSf) and poly(acrylic acid) (PAA) membranes were prepared as follows: (i) PSf (17 g) was completely dissolved in DMF solvent (83 g) at 90 °C, and then appropriate weights of PAA powder were added to the PSf solutions in order to obtain different membrane compositions (Table 1); (ii) at room temperature, the de-bubbled polymer solution was cast on a glass plate with a lab-made casting knife with a gap set to 200 μm. The cast liquid-film was left for evaporation in air for 20 s before its immersion in a water coagulation bath (MilliQ water, 18.2 MΩ cm, pH 5.8 and the TOC 2.1 mg/L) at 18 °C. A white solid film stripped out of the glass plate little moment after immersion. The coagulated membranes were abundantly washed with water and stored in sodium azide solution. The obtained membranes exhibited a shiny surface on the water-bath side, which is the side of the dense layer, and a dull surface on the glass support side.

2.3. Ion exchange capacity measurement

The ion exchange capacity was determined after alternative sample conditionings in NaOH 0.1 M and HCl 0.1 M for an immersion time of at least 4 h. In H^+ form, the sample was equilibrated in water for at least 12 h to remove the free hydrogen ions. Afterwards the membranes in carboxylic form were immersed for 4 h, in 100 ml of mixed solution containing NaOH (0.025 mol/L) and NaCl (0.075 mol/L). The amount of –COOH groups was determined by back titration with HC1 0.01 M.

2.4. Scanning electronic microscopy and the electron dispersive X-rays

The membrane surfaces and sections were analyzed by a Zeiss EVO 40 EP microscope with the Secondary Electron Backscattered Detector (CE-BSD). Samples were frozen in liquid nitrogen at 190 °C, fractured and coated with a thin gold film. SEM observations were carried out at various magnifications while the electron beam energy was fixed at 10 keV. Micrographs of scanning electron microscopy with an energy dispersive X-rays (SEM-EDX) were done at an accelerating voltage of 15 kV and an X-rays analysis counting time of 150 s. Multiple areas (6–9 zones) of each membrane surface were selected to collect the SEM-EDX spectrum.

2.5. FTIR measurement

Prior to the spectra recording, membranes were placed in a vacuum oven at 80 °C for 48 h to evaporate solvent and non-solvent traces. FTIR films spectra were recorded in the range of 700–4000 cm^{-1}, by averaging 64 scans at a resolution of 4 cm^{-1}, by means of a Nicolet AVATAR 360 FT-IR Spectrometer in the attenuated total reflectance (ATR) mode (with the ATR Omni-sampler device). The analyzed face was firmly pressed against the crystal surface in the ATR device. In this mode, the infrared evanescent wave penetrates the sample from the surface down to a depth of about 2 μm.

2.6. Porosity evaluation

Butanol was used to determine the overall porosity of PSf/PAA membranes. This parameter was calculated as following [38,39]:

$$P\ (\%) = 100\frac{W_w - W_d}{\rho_w}V$$

where W_w is the weight of wet membranes (g), W_d is the weight of dry membranes (g), ρ_w is the density (g/cm^3) of butanol, and V is the volume of the membrane in wet state (cm^3). Membrane thickness was measured by a digital micrometer at multiple-points in order to calculate a correct average value.

Table 1
Composition of the casting solutions (weight) and the PSf/PAA proportions after the elimination of solvent; the thickness of the top skinned layer, ion exchange capacity, porosity and hydraulic permeability of PSf/PAA as a function of PSf/PAA proportions.

Sample	m_{PSf} (g)	m_{PAA} (g)	m_{DMF} (g)	PSf/PAA	e (nm)	Lp (L/(m^2 h bar))	C_p (mequiv./g)	P
J_0	17	0.000	83	100/0	180 ± 2	1.4	0.0	36.2
J_1	17	0.720	83	96/04	187 ± 2	40	1.19	33.4
J_2	17	1.475	83	92/08	212 ± 2	23	1.29	34.1
J_3	17	2.130	83	89/11	1494 ± 2	9	1.37	33.2
J_4	17	3.100	83	85/15	–	–	–	29.0

Composition of PSf/PAA dope casting and some properties of their films, the top skinned layer thichness e (nm), the hydraulic permeability L_p (L/(m^2 h bar)), ion exchange capacity C_p (mequiv./g of dried membrane) and the overall porosity P.

2.7. Permeation measurements

Dead-end filtration was done with stirred Amicon 401S cell with effective area of 0.0038 m^2. It was thermostated at 25 °C. Flux values of pure water and metal ion solutions at different transmembrane pressures (ranging 0–0.4 MPa) were measured at steady state condition using Eq. (2):

$$J_v = \frac{\Delta V}{S\,\Delta t} \tag{2}$$

where J_v is the volume flux (L/(m^2 h)), ΔV is the variation of permeate volume (L), S is the membrane effective area (m^2), and Δt the time interval (h). The hydraulic permeability was calculated from the Poiseuille's law as represented with Eq. (3):

$$P_m = \frac{J_v}{\Delta P} \tag{3}$$

where P_m is the hydraulic permeability (L/(m^2 h MPa)) and ΔP is the transmembrane pressure (MPa). For the retention of heavy metal ions, all filtration experiments were done with 150 ml of solution at stirrer speed of 10 rps (600 rpm). The first 7 ml permeate was discarded and the subsequent volumes were collected for analysis. Before each dead-end filtration experiment under magnetic stirring, the membrane was exposed to a higher pressure (5 bar) to stabilize them.

Observed rejection (R_o) is usually used to characterize the solute transmission through membranes. It is calculated according to Eq. (4):

$$R_o\,(\%) = 100\left(1 - \frac{C_p}{C_b}\right) \tag{4}$$

where C_p and C_b are the solute concentrations in permeate and in the feed, respectively. R_o depends on the pH, the salt concentration and the system hydrodynamics which may be characterized by the Reynolds number R_e and the mass transfer coefficient k [40]. For a stirred cell, $R_e = \omega r^2/\nu$, with ν is the kinematic viscosity, ω is the stirring speed in round-per-second (10 rps), and r is the radius of the stirred cell (r = 0.0348 m). For the dilute salt solutions, the values for the kinematic viscosity ν were practically equal to that of water, i.e. 10^{-6} m^2/s. A value of 10^{-10} m^2/s was taken for the salt diffusion coefficient (under-estimated value). The calculated Reynolds number, R_e = 14,440, shows that experiments were done under turbulent conditions.

The mass transfer coefficient k can be derived from an experimentally derived correlation [40] between the value of the R_e and that of the Schmidt number Sc:

$$\frac{k\,r}{D_\infty} = \phi\, R_e^{0.567}\, Sc^{0.33}$$

$Sc = \nu/D_\infty$, with D_∞ the diffusion coefficient at infinite dilution. The parameter ϕ is a function of device geometry of the used stirred cell (0.4). This gave a mass transfer coefficient k of 5×10^{-6} m/s. This value is rather high due to the turbulence regime and the high salt diffusivity. Thus, we considered that the analysis of the change in the observed rejection in different studied cases based on the observed rejection reflect well that of the true rejection.

The membrane regenerations were performed by immersing successively the sample into a stirred HNO_3 0.1 M solution for 30 min, and sodium hypochlorite solution of 1.3% of active chlorine (30 min), then repeatably in water. HNO_3 solution was used to remove heavy metal ions. Sodium hypochlorite cleaned the membrane by removing organic contaminants clogging the membrane pores. After such a treatment, membrane recovered approximately its initial hydraulic permeability and retention properties (with ± 5% fluctuations).

2.8. Atomic absorption spectroscopy measurements

Concentration of metal ions was measured by atomic absorption spectroscopy and the pH of feed solutions was adjusted to the desired pH by adding small volumes of NaOH 1 M before the permeation process. The apparatus was a Varian Spectre AA-100B Atomic Absorption Spectrophotometer (Mulgrave, Australia) operating with an air-acetylene flame as atom generator and monitored by the SpectrAA version 4.10 software. Lead was analyzed by using a Photron monoelement hallow cathode lamp in the following conditions: the wavelength and slit width were respectively 217 nm and 1 nm for lead; 326.1 nm and 0.5 nm for cadmium and 429 nm and 0.5 nm for chromium. Standard concentration ranges were 0–25 mg/L for lead, 0–10 mg/L for cadmium and 0–10 mg/L for chromium. Each solution was measured in triplicate with a RSD < 3%. The concentration of each sample was deduced directly from the calibration curves or corrected by the dilution factor in case of concentration over-range.

3. Results and discussion

3.1. Membrane characterization

3.1.1. PAA immobilization into PSf networks

The presence of PAA on the membrane surface or in the matrix is important for metal-ion retention. Fourier transform infrared (FTIR) as well as the determination of ion exchange capacity were used to evaluate the efficiency of PAA immobilization in PSf networks. The surface on the skin side of the blend membranes with PAA contents of 0%, 10% and 15%, respectively, were analyzed by FTIR-Atr spectroscopy. Fig. 1 shows the spectra of PSf and PSf/PAA membranes in the range of 1600–1800 cm^{-1}. The new peak at 1720 cm^{-1} in the PSf/PAA membrane spectra, that can be assigned to the streaching vibration of C=O group, indicates the presence of PAA in the blend

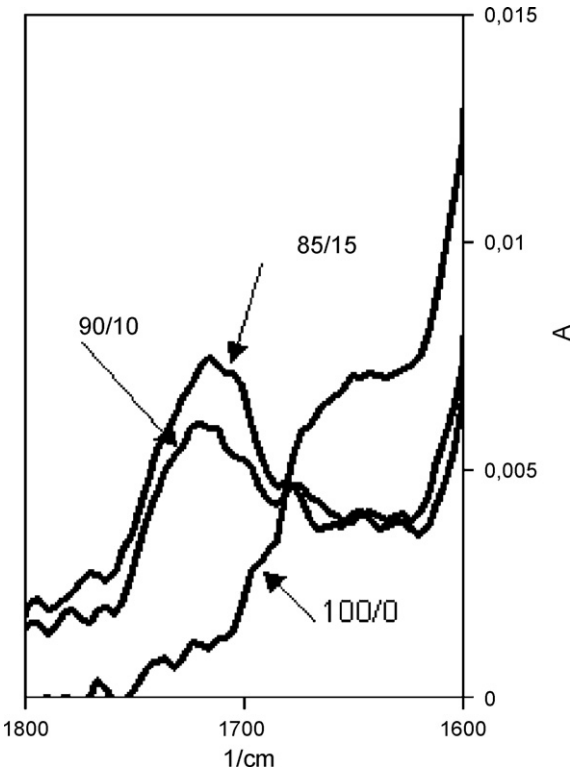

Fig. 1. FTIR spectrum of PSf/PAA 100/0, 90/10 and 85/15 in the range 1600–1800 cm^{-1}.

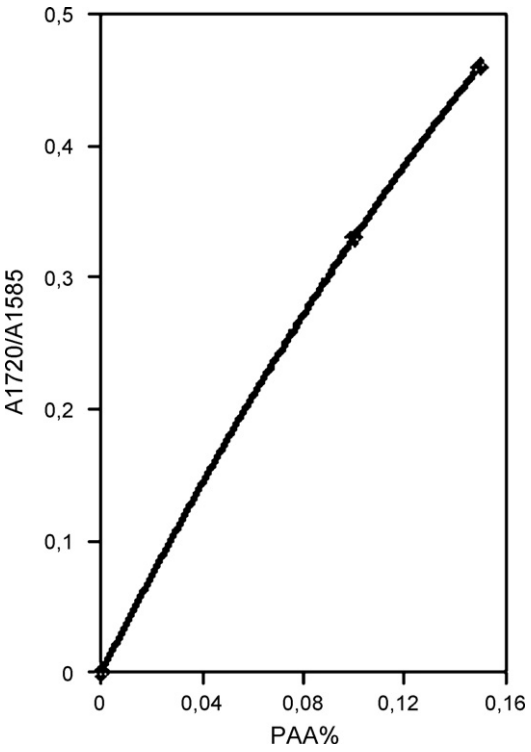

Fig. 2. Ratio A_{1720}/A_{1585} as a function of the PAA content in casting solution.

membrane. Using the peak of C=C double bond [41] observed at 1585 cm^{-1} as a reference, the ratio of the absorbance of carbonyl group 1720 cm^{-1} to the double bond peak 1585 cm^{-1} (A_{1720}/A_{1585}) was used to quantify the PAA immobilization in the PSf matrix. The increase in membrane-immobilized PAA with the increase in PAA content in the casting dope, as shown in Fig. 2, is confirmed by the similar variation trend in the ion exchange capacity (Table 1). It should be noted that FTIR-Atr spectroscopy gave an image of chemical structure of the membrane surfaces, while the ion exchange capacity represents the overall content in carboxylic acid in the whole membrane.

Anyway, these results prove that the PAA polymer, in spite of its water solubility, is well immobilized in the PSf matrix. The quantity of immobilized PAA increases with the increase of its content in the casting dope. It can be proposed that the PAA chains that are entangled with PSf chains and bound by interactions in the casting dope would be kept with PSf in the polymer-rich phase, when the liquid/liquid phase separation occurs. The vitrification of the polymer components would prevent the PAA extraction into the external aqueous phase. Although the PSf matrix is not chemically cross-linked, the interactions in the matrix are strong enough to maintain the matrix in a physically cross-linked state that practically immobilizes PAA chains. One may wonder whether PAA chains can leak through the PSf network. As result, our blend membranes were experimentally, stable for months, without significant PAA leak. Although a repitition of PAA chains towards an external aqueous is possible under a chemical driving force, the PAA chains would form snares at different fixed points of the network that make impossible net movement of the chains.

3.1.2. Scanning electron microscopy results

The scanning electron microscopy was used to collect information regarding membrane morphology. Fig. 3 shows the images of the top-surface of PSf/PAA 100/0, 96/04, 92/08 and 89/11 respectively whereas Fig. 4 shows the cross-section morphologies of PSf/PAA 89/11 membrane. The measurement of skin-layer thick-

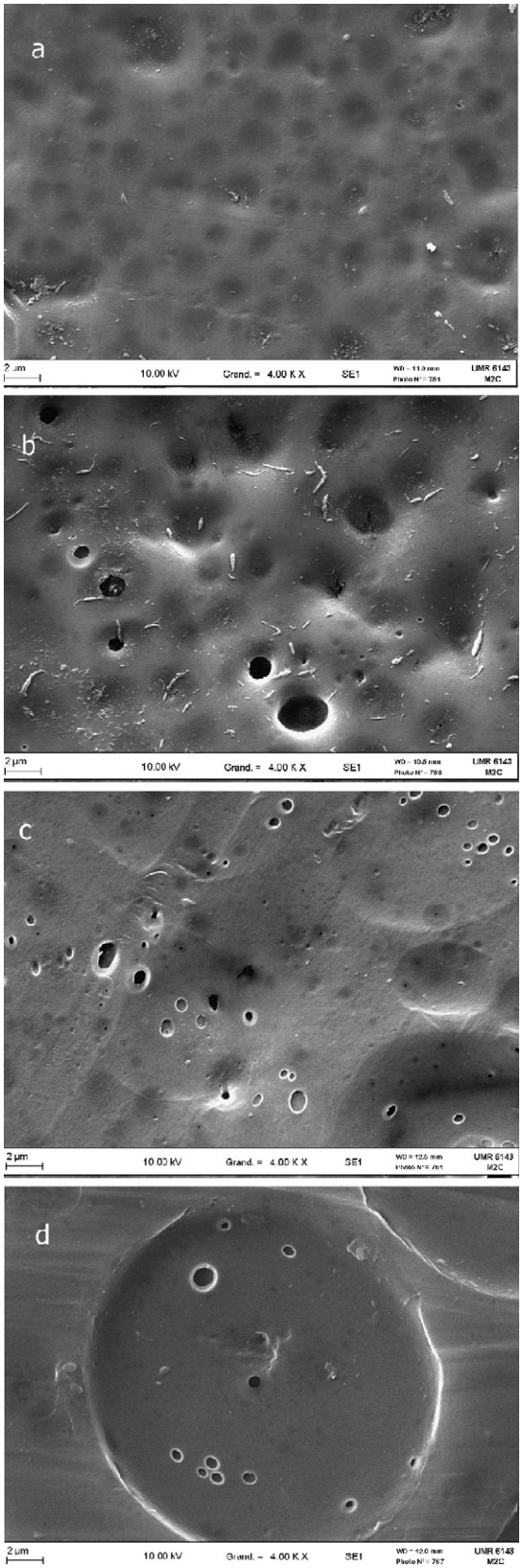

Fig. 3. SEM top-surface of PSf/PAA membranes (4000× magnitude): (a) PSf/PAA 100/0, (b) PSf/PAA 96/04, (c) PSf/PAA (92/08) and (d) PSf/PAA 89/11.

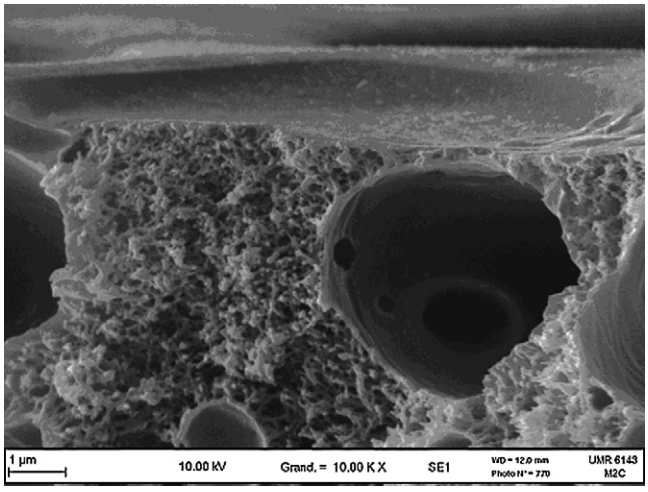

Fig. 4. SEM cross-section of PSf/PAA 89/11 membranes (10,000× magnitude).

ness has shown the thickenning of this layer with the increase of PAA content as already summarized in Table 1.

SEM images of the membrane surfaces, reveal that membranes contain inter-connected or dead-ended pores with different densities and sizes according to the PAA content. It was also observed that the outer-surface pores contain sub-open pores and fine pores inner the sub-pores. For instance, the measurement of the pore diameters on the SEM images of PSf/PAA 92/08 revealed that the mean pore size of the outer-surface pores, sub-structure open pores and fine pores inner the sub-structure were 680 nm, 136 nm and 25 nm, respectively. In fact, in pressure-driven membrane processes, the transmembrane flux and selectivity are governed by the fine interconnected pores where there is the main resistance to flow and sieving action, while the sub-structure with large pores provides the membrane with a correct mechanical resistance.

In so far as the sub-structure has a low enough hydraulic resistance with respect to the fine-pore region, too-big pores (finger-like macrovoids) are not desired in order to avoid hydraulic permeability alteration by compaction in filtration operations. Generally, it was found that the membrane morphology changes from finger (or macrovoids) to sponge-like structures with the increase of polymer concentration or with the addition of second polymer as polyvinylpyrrolidone (PVP) [42]. A similar trend was observed for PSf/PAA membranes with the increase in PAA content, and may be attributed to the delay of phase separation due to the addition of hydrophilic polymer (PAA) to the casting dope.

3.1.3. Membrane porosity, P

Table 1, shows a slight decrease in the PSf/PAA membrane porosity (P) when the PAA fraction in the casting dope of blend polymers increases, while the PSf content is maintained constant. Such a result is consistent with the SEM images which show the decrease of pore sizes and the increase of the thickness of skin layered with the increase of PAA content. It should be noted that with the increase of PAA fraction in the dope solutions, at constant PSf content, the total polymer concentration in the dope medium increases. Thus, the logical consequence is a more compact membrane structure obtained in coagulation, because of a higher density of polymer chains that are coagulated by the water bath [41].

3.1.4. Hydraulic permeability L_p and polymer retention characteristics

The hydraulic permeability (L_p) of pure water across PSf/PAA membrane decreases with the increase in PAA content (Table 1), as a result of the above-mentioned porosity decrease in the membrane. Since all membranes were stabilized at 0.5 MPa for more than 6 h prior to the permeability measurement, the measured water permeability were the intrinsic permeability that reflects membrane porous structure: interconnectivity, pore size and distribution.

The hydraulic permeability of the membranes of different PAA content is qualitatively consistent with the membrane morphology and porosity. The decrease in the hydraulic permeability, when the PAA content increases, can be related to the thickening of the dense skin, to the decrease of pore sizes and to the porosity reduction. The PSf membrane containing small PAA amount (4%) had a similar skin-layer thickness as the PSf membrane without PAA as shown in Table 1. Much higher hydraulic permeability observed for the PSf membrane containing a small PAA amount is due to the larger pore sizes.

3.2. Membrane performances in the removal of heavy metal

For the purpose of heavy metal removal, fast screening tests were performed with a lead nitrate solution in standard filtration conditions. They led us to select the PSf/PAA 89/11 blend membrane for the target application. This membrane exhibited the best heavy metal retention because of its high content in PAA (1.37 mequiv./g) and their smaller pore sizes. The use of the total organic carbon (TOC) techniques for the ultrafiltration of different molecular weight of polyethylene glycol, in aqueous solution 1 g/L, has shown that the molecular weight cut-off (MWCO) of the selected membranes was ca. 10,000 g/mol under 0.2 MPa. The PSf/PAA 89/11 blend membrane was thus chosen for the study of heavy metal removal from water by ultrafiltration process. Moreover, the calculation of Reynolds number R_e and mass transfer coefficient k, as explained in experimental section, prove that experiments were done under turbulent conditions and the observed ions rejection is nearly equal to the real ions rejection.

3.2.1. Study of membrane—lead ion interactions by SEM-EDX technique

Scanning electron microscopy with an energy dispersive X-rays (SEM-EDX) or electron dispersive spectroscopy (EDS) can afford spatial and composition distribution of elements in solid materials. Elements with higher atomic number generate more backscattered electrons, thus appear in SEM-EDX images brighter than those of low atomic number [43]. Soluble metal ions have a hydrated size in solution much smaller than that of the water-soluble polymers used to estimate the sieving effect of the pores of ultrafiltration membranes, thus generally pass through the membrane without retention. We infer that other mechanism than the pore sieving effect governs the lead ion retention in filtration. Such a mechanism may be a fixation of lead ions on the membrane by interactions with the carboxylate groups. SEM-EDX was used to highlight such a fixation of lead ions onto the skin of the PSf/PAA 89/11 membrane. SEM-EDX topographic images of the top surface of PSf/PAA 89/11 membrane after ultrafiltration of a $Pb(NO_3)_2$ solution were taken on a non-washed part (Fig. 5b) and on a 2 h-washed (with MQ water) part (Fig. 5c) of the membrane sample. These images show bright zones, with different sizes, whose number and size are greater for the non-washed sample. The bright zones on the surface of the washed membrane correspond to the complexed lead-ions, that a thorough washing was not able to remove its from the surface (Fig. 5b and c). Indeed, the EDX spectrum (Fig. 5d) of the bright zones, in washed sample, highlight the presence of lead, at lead-atom characteristic X-ray emissions: M_α at 0.234 and M_β at 0.245 KeV of energy. As PSf alone cannot fix the lead ion, which is completely soluble in the used operating conditions, we infer that the fixed (or complexed) ions are due to the presence of PAA carboxyl groups on the surface of the PSf/PAA membrane.

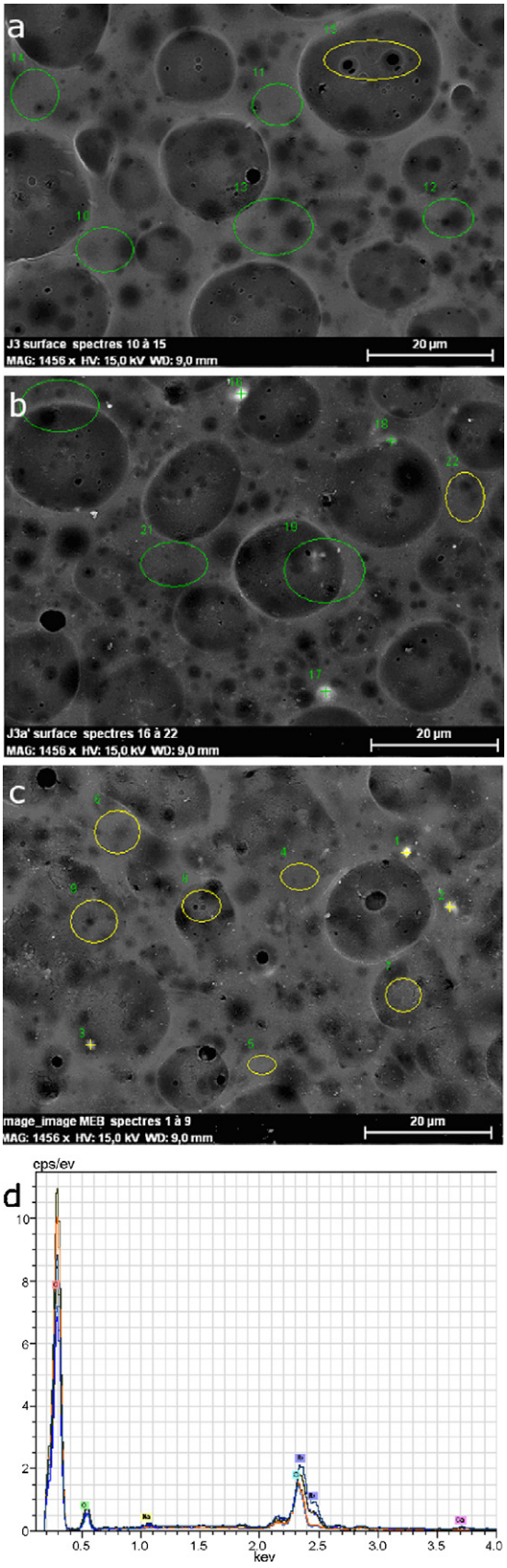

Fig. 5. SEM-EDX spectra of the top surface of PSf/PAA 89/11 membranes (a) before filtration of $Pb(NO_3)_2$, (b) after filtration without membrane washing, and (c) after filtration with membrane washing. (d) EDX spectrum of the membrane top surface after washing. Concentration of the $Pb(NO_3)_2$ solution was 20 mg/L and its pH was 4.98. The cross-flow filtration was effected under 0.2 MPa, 600 rpm and 25 °C.

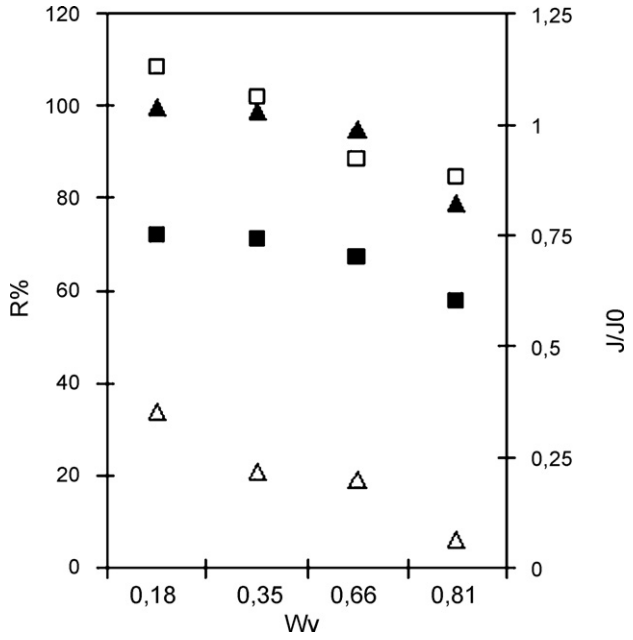

Fig. 6. Retention ratio (R%) (△: pH 3.5; ▲: pH 5.7) and normalized flux (J/J_0) (□: pH 3.5; ■: pH 5.7) of lead ions as a function of permeate volume fraction (W_v) at P = 0.2 MPa, 600 rpm and $[Pb^{2+}]$ = 20 mg/L.

3.2.2. Study of the retention of heavy metal ions by PSf/PAA membranes

3.2.2.1. Influence of the pH of feed solution on membrane performance.

Lead nitrate solutions at pH 3.5 and pH 5.7 were batch-ultrafiltrated through the PSf/PAA membrane at constant pressure. These pH values were chosen to obtain the membrane carboxylic groups in two distinct ionization states, a non-ionized acid form at the lower pH and a mainly ionized form at the higher pH. In fact, Fig. 6 shows the retention of lead ion as a function of permeate volume fraction (W_v) is always better at higher pH. This behavior can be explained as follows: polysulfone is a hydrophobic material with negligible interactions with ions; whereas PAA is a hydrophilic material with carboxylic groups which have both ion exchange and complexation abilities (cross-linked PAA beads are often used as weak cation-exchange resins). At low pH, the carboxylic groups in the acid form are involved in hydrogen bonds which reduce their ion–ion interactions with metal ions. As a result, the soluble lead ions pass easily through the membrane leading to a low retention. The small lead ions retention at low pH may be attributed to membrane morphology (dead-pores) and weak dipole-ion interactions between carboxylic acid groups and lead ions ($-OH\cdots M^{n+}$). At higher pH, the carboxylic group of PAA in the membrane is more ionized and more capable of metal-ion complexation or ionic interactions ($^{-}O\cdots M^{n+}\cdots O^{-}$). The observed decrease in the retention with the increase in permeate volume fraction is a direct consequence of the concentration build-up in the feed compartment due to the ion retention, since the initial feed concentration in lead ion was taken as reference in the retention ratio.

Normalized flux of lead-solution through the PSf/PAA membrane appears to be always higher for the solution at pH 3.5 than for the solution at pH 5.7 (Fig. 6). This situation is not quite usual, and not easy to interpret. It should be noted that the solutions had practically the same viscosity as pure water so that there should be no additional friction loss in the permeate transport by convection in the membrane pores. As a soluble ion, lead has a much larger diffusion coefficient than macromolecules. Given the low concentration, we can expect negligible concentration polarization. Explications of the higher permeate flux at pH 3.5 are to be found in a change in

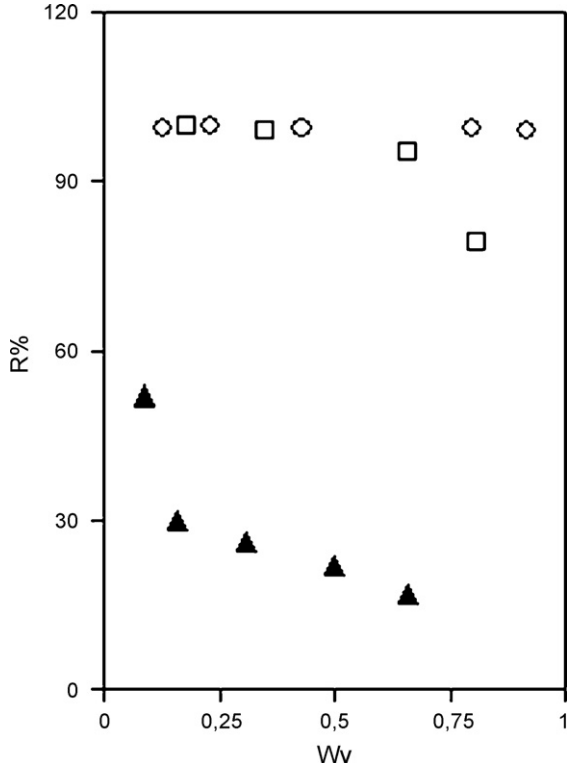

Fig. 7. Retention ratio (R%) of lead ions as a function of permeate volume fraction (W_v) at different [Pb^{2+}] = 10 mg/L (○), 20 mg/L (□) and 30 mg/L (▲) (P = 0.2 MPa, pH 5.7, 600 rpm).

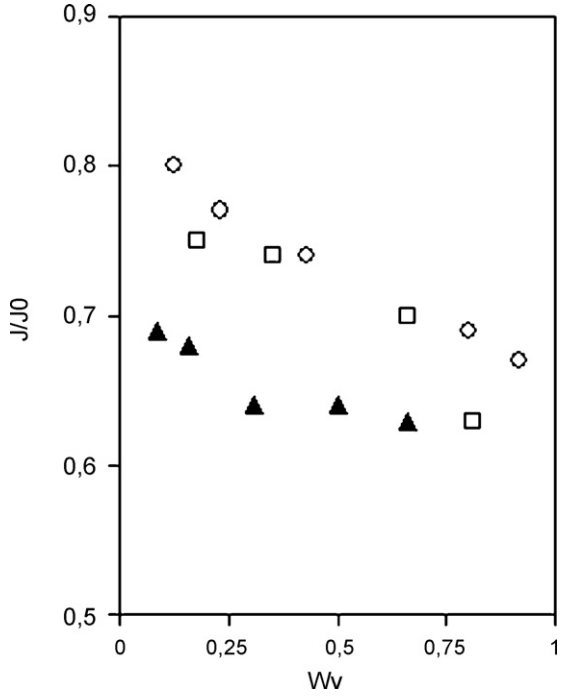

Fig. 8. Normalized flux (J/J_0) of lead ions as a function of permeate volume fraction (W_v) at P = 0.2 MPa, pH 5.7, speed stirring 600 rpm and various feed concentrations Pb^{2+} = 10 mg/L (○), 20 mg/L (□) and 30 mg/L (▲).

the membrane properties with pH. It must be kept in mind that PSf/PAA membrane contains PAA with carboxylic acid groups in its matrix. At the higher pH, the acid groups become ionized, and the repulsion between segments bearing the same charges with ionization groups would expand the chain segments into the solution into pores. At low pH, these groups tend to coil back into a collapsed form due to the formation of hydrogen bonds. It can be expected from such a change in the PAA conformation with pH that pore diameter increases when the pH of the permeating fluid decreases. The complexation or ion exchange of lead ion neutralizes part of the carboxylate charged groups in the pores, but also adds matters to the pore inner wall. As a consequence, the permeation flux is higher at lower pH.

3.2.2.2. Influence of the concentration and total pressure of feed solution on membrane performance. Fig. 7 shows the variation of the lead ion retention as a function of permeate volume fraction at different concentrations. The curves show a decrease in the retention ratio with the increase in feed concentration and with the increase of permeates volume.

In fact, at low concentrations, the PSf/PAA membrane exhibited a high retention capacity. This performance decrease with the increase of the lead-ion concentration can be related to the tendency of the ionic groups on the membrane to be saturated when the lead-ion concentration in the feed increases (for the same permeate volume extracted through the membrane).

Normalized permeation flux decreases with the increase in feed concentration as shown in Fig. 8. Such a behavior can be interpreted as a consequence of increase in the number of lead ion fixed on the pore wall, which tends to reduce the free pore-volume and the permeation flux through the membrane.

Fig. 9 shows the variation of lead ions retention and normalized flux as a function of permeate volume at different pressures. It appears that for the first permeate volume (25% of feed volume) the lead retention is independent on the feed pressure; the retention ratio is almostly 100%. But with the increase of permeate volume, which is associated with an increase of feed concentration (batch process), lead retention decreases. Such a behavior is more important for the higher initial feed pressure.

Otherwise, the normalized flux increases with the increase of pressure and decreases with the increase of permeate volume whatever the variation of pressure. As observed previously, at pH 5.7, lead ions are easily fixed by membrane charges (carboxylate groups). This fixation disturbs the solute permeation through the membrane as the pore sizes reduce. The association between solute and membrane charge are enhanced by the decrease of feed pres-

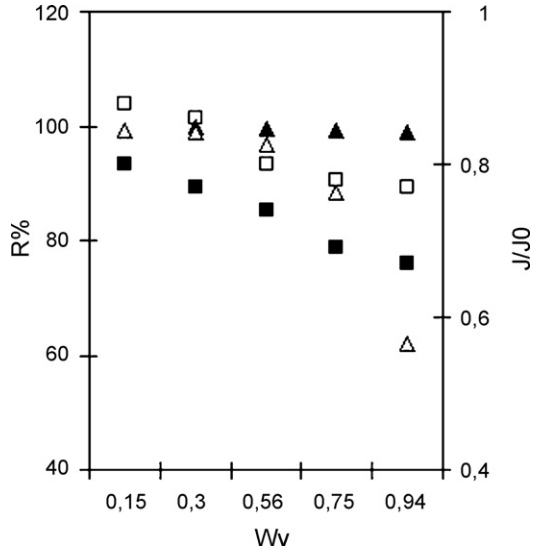

Fig. 9. Retention ratio (R%) (▲: 0.2 MPa; △: 0.35 MPa) and normalized flux (J/J_0) (■: 0.2 MPa; □: 0.35 MPa) of lead ions as a function of permeate volume fraction (W_v) at fixed speed stirring 600 rpm, pH 5.7 [Pb^{2+}] = 10 mg/L.

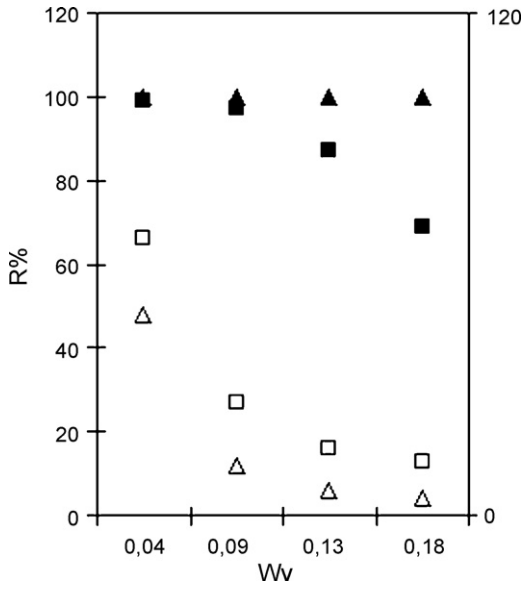

Fig. 10. Retention ratios (R%) of cadmium ions (□: pH 2.5; ■: pH 5.8) and of chromium ions (△: pH 3.2; ▲: pH 5.8) as a function of permeate volume fraction (W_v) at P = 0.05 MPa, 400 rpm and $[Cd^{2+}] = [Cr^{3+}] = 10$ mg/L.

sure. In fact, the contact-time between membrane charges and permeate metal ions is longer at low pressure.

3.2.2.3. Cadmium and chromium ions removal as a function of pH. Fig. 10 illustrated the variations of retention ratio of cadmium ions (Cd^{2+}) solution of 10 mg/L through PSf/PAA membrane at pH 2.5 and 5.8, and that of chromium (Cr^{3+}) solution of 10 mg/L at pH 3.2 and 5.8. They are consistent with those for lead ions. At low pH, the metal ion retentions are very low because of the carboxylic groups in acid form. In the opposite case, at high pH, these groups are in ionized form.

The high metal retentions in spite of the larger size of pores compared with that of the metal ions (whose radii for their hydrated form are 0.43 nm, 0.426 nm and 0.45 nm for lead, cadmium and chromium, respectively) suggest that the permeation path through the membrane is highly tortuous, so that the transport ions have a high probability to be caught by the carboxylate groups on the pore walls. We speculate that hydrophilic groups of poly(acrylic acid) are attracted by the penetrated water molecules (non-solvent) during the coagulation process. This attraction induces an arrangement of hydrophilic groups at the interfaces of the formed tortuous pores. This preferential distribution of carboxylic groups on the pore wall would cause the high metal ion retention by the membrane.

The large range of electrostatic interactions between ions and membrane charges was reported in many works [44,45]. These electrostatic interactions have been mainly classified in two types: short-range and long-range. In the former the movements of counter ions (metal ions) are completely hindered while in the later it is slightly hindered. If the ions can come closer on its convective pathway, they would be completely blocked.

On the basis of the literature results [44,45] it can be expected that, the metal ions participate in long-range and short-range interactions with the carboxyl groups on the pore surfaces and in the membrane matrix. These electrostatic interactions which depend on pH, on ionic strength and on the nature of the permeating species, induce the complexation of heavy metal ions and their retention from the filtered water. Nevertheless, it is not possible for us to quantify the contribution of each type of interactions, as it depends on numerous factors (local pH and concentrations, local polymer conformations, etc.).

The high metal rejection, at pH ≥ 5.7, leads us to suggest that the complexation between metal ions and carboxylate groups ($-COO^-$) on the inner surface of pores and membrane matrix act as an electrostatic repulsion barrier against the non-complexed metal ions.

Brian et al. [46] suggested that the high rejection of divalent ions (as calcium ions (Ca^{2+})), by membrane composed of polystyrene sulfonate sodium deposited onto porous alumina support, is mainly due to the positive charged layer created by the adsorption of Ca^{2+}. Our results are consistent with this mechanism of rejection enhancement.

4. Conclusion

The use of ultrafiltration-ion exchange membrane with semi-interpenetrating polysulfone (PSf) and polyacrylic acid (PAA) network to remove lead, chromium and cadmium from water has shown excellent results mainly at pH superior than 5.7. Immobilization of PAA in PSf matrix was demonstrated by Fourier transform infrared and the ion exchange capacity measurements. Efficiency of lead, chromium and cadmium retention, from water, increases with pH increase. The high retention was attributed to the complexation between metal ions and carboxylate groups ($-COO^-$) on the inner surface of pores and membrane matrix. Moreover, the membrane–solution interactions are found to be the origin of the hydraulic permeability changes.

It is worth noting that these membranes may offer several advantages due to the repartition of their charges over the whole membrane matrix. They may be used for the deposition of polyelectrolyte layers and for the ultrafiltration assisted by complexation. For both processes, they would offer best results as they constitute a second barrier to remove metal ions.

Acknowledgement

We would like to thank the France government (SCAC Amprun project, Nouakchott, Mauritania) for the financial support that help us to achieve this work.

References

[1] M. Ulbricht, Advanced functional polymer membranes, Polymer 47 (2006) 2217–2262, (feature article).
[2] M. Peter-Varbanets, C. Zurbrügg, C. Swartz, W. Pronk, Decentralized systems for potable water and the potential of membrane technology, Water Res. 43 (2009) 245–265.
[3] S.K. Sikdar, D. Grosse, I. Rogut, Membrane technologies for remediating contaminated soils: a critical review, J. Membr. Sci. 151 (1998) 75–85.
[4] Y. Sato, M. Kang, T. Kamei, Y. Magara, Performance of nano filtration for arsenic removal, Water Res. 36 (2002) 3371–3377.
[5] L.A. Pereira, G.I. Amorim, J.B. Borba da Silva, Development of methodologies to determine aluminium, cadmium, chromium and lead in drinking water by ET AAS using permanent modifiers, Talanta 64 (2004) 395–400.
[6] Q.W. Yang, W.S. Shu, J.W. Qiu, H.B. Wang, C.Y. Lan, Lead in paddy soils and rice plants and its potential health risk around Lechang lead/zinc mine, Guangdong, China, Environ. Int. 30 (2004) 883–889.
[7] M.G. Mayer, D.N. Wilson, Health and safety—the downward trend in lead levels, J. Power Sources 73 (1998) 17–22.
[8] M. Berthier, O. Kremp, Saturnisme: le nouveau rôle du pédiatre, Arch. Pédiatr. 7 (2000) 919–923.
[9] Y. Seid, Y. Nakano, Y. Nakamura, Rapid removal of lead of dilute lead from water by pyroaurite-like compound, Water Res. 35 (2001) 2341–2346.
[10] E. Fischer, C.M.G. van den Berg, Determination of lead complexation in lake water by cathodic stripping voltammetry and ligand competition, Anal. Chim. Acta 432 (2001) 11–20.
[11] K. Güçlü, R. Apak, Modeling of copper (II), cadmium (II), and lead (II) adsorption on red mud from metal–EDTA mixture solutions, J. Colloid Interface Sci. 228 (2000) 238–252.
[12] B.L. Rivas, E.D. Pereira, I.M. Villoslada, Water-soluble polymer–metal ion interactions, Prog. Polym. Sci. 28 (2003) 173–208.
[13] I. Korus, M. Bodzek, K. Loska, Removal of zinc and nickel ions from aqueous solutions by means of the hybrid complexation–ultrafiltration process, Sep. Purif. Technol. 17 (1999) 111–116.

[14] B.R. Fillipi, L.W. Brant, J.F. Scamehorn, S.D. Christian, Use of micellar-enhanced ultrafiltration at low surfactant concentrations and with anionic–nonionic surfactant mixtures, J. Colloid Interface Sci. 213 (1999) 68–80.
[15] J. Landaburu-Aguirre, V. García, E. Pongrácz, R.L. Keiski, The removal of zinc from synthetic wastewaters by micellar-enhanced ultrafiltration: statistical design of experiments, Desalination 240 (2009) 262–269.
[16] B.R. Fillipi, J.F. Scamehorn, S.D. Christian, R.W. Taylor, A comparative economic analysis of copper removal from water by ligand-modified micellar-enhanced ultrafiltration and by conventional solvent extraction, J. Membr. Sci. 145 (1998) 27–44.
[17] M. Bodzek, I. Korus, K. Loska, Application of the hybrid complexation-ultrafiltration process for removal of metal ions from galvanic wastewater, Desalination 121 (1999) 117–121.
[18] P. Canizares, A. Pèrez, R. Camarillo, Recovery of heavy metals by means of ultrafiltration with water-soluble polymers: calculation of design parameters, Desalination 144 (2002) 279–285.
[19] B.L. Rivas, I. Moreno-Villoslada, Prediction of the retention values associated to the ultrafiltration of mixtures of metal ions and high molecular weight water-soluble polymers as a function of the initial ionic strength, J. Membr. Sci. 178 (2000) 165–170.
[20] I. Moreno-Villoslada, B.L. Rivas, Retention of metal ions in ultrafiltration of mixtures of divalent metal ions and water-soluble polymers at constant ionic strength based on Freundlich and Langmuir isotherms, J. Membr Sci. 215 (2003) 195–202.
[21] A. Aliante, N. Bounatiro, A.T. Cherif, D.E. Akretche, Removal of chromium from aqueous solution by complexation-ultrafiltration using a water-soluble macroligand, Water Res. 35 (2001) 2320–2326.
[22] J. Müslehiddinoglu, Y. Uludag, H.Ö. Özbelge, L. Yilmaz, Effect of operating parameters on selective separation of heavy metals from binary mixtures via polymer enhanced ultrafiltration, J. Membr. Sci. 140 (1998) 251–266.
[23] J. Barron-Zambrano, S. Laborie, Ph. Viers, M. Rakib, G. Durand, Mercury removal from aqueous solutions by complexation-ultrafiltration, Desalination 144 (2002) 201–206.
[24] A. Kryvoruchko, L. Yurlova, B. Kornilovich, Purification of water containing heavy metals by chelating-enhanced ultrafiltration, Desalination 144 (2002) 243–248.
[25] M.R. Pastof, E.S. Vidalb, P.V. Galvhnb, D.P. Ricoa, Analysis of the variation in the permeate flux and of the efficiency of the recovery of mercury by polyelectrolyte enhanced ultrafiltration (PE-UF), Desalination 151 (2002) 247–251.
[26] J. Llorens, M. Pujolà, J. Sabaté, Separation of cadmium from aqueous streams by polymer enhanced ultrafiltration: a two-phase model for complexation binding, J. Membr. Sci. 239 (2004) 173–181.
[27] A. Maartens, P. Sward, E.P. Jacobs, Feed water pretreatment: methods to reduce membrane fouling by natural organic matter, J. Membr. Sci. 163 (1999) 51–62.
[28] D. Moeckel, E. Staude, M. Dal-Cin, K. Darcovich, M. Guiver, Tangential flow streaming potential measurements: hydrodynamic cell characterization and zeta potentials of carboxylated polysulfone membranes, J. Membr. Sci. 145 (1998) 211–222.
[29] Y. Matsumoto, M. Sudoh, Y. Suzuki, Preparation of composite UF membranes of sulfonated polysulfone coated on ceramics, J. Membr. Sci. 158 (1999) 55–62.
[30] M.D. Guiver, G.P. Robertson, M. Yoshikawa, C.M. Tam, Funtionalized polysolfones: methods for chemical modification and membrane applications, membrane formation and modification, in: ACS Symposium Series, vol. 744, American Chemical Society, Washington, DC, 2000, pp. 137–161.
[31] D. Mockel, E. Staude, M.D. Guiver, Static protein adsorption, ultrafiltration behavior and cleanability of hydrophilized polysulfone membranes, J. Membr. Sci. 158 (1999) 63–75.
[32] J.K. Fang, H.C. Chiu, J.Y. Wu, S.Y. Suen, Preparation of polysulfone based cation-exchange membranes and their application in protein separation with a plate and frame nodule, React. Funct. Polym. 59 (2004) 171–183.
[33] L. Breitbach, E. Hinke, E. Staude, Heterogeneous functionalizing of polysulfone membranes, Die Angewandte Makromolekulare Chemie 184 (1991) 183–196.
[34] P. Zschocke, D. Guellmalze, Novel ion exchange membrane based on an aromatic polyethersulfone, J. Membr. Sci. 22 (1985) 325–332.
[35] O. Olabisi, L.M. Robeson, M.T. Show, Polymer–Polymer Miscibility, Academic Press, New York, 1979.
[36] Y. Osada, T. Nakagawa, Membrane Science and Technology, Marcel Dekker Inc., New York, 1992.
[37] C.O. Mbareck, Q.T. Nguyen, S. Alexandre, I. Zimmerlin, Fabrication of ion-exchange ultrafiltration membranes for water treatment. I. Semi-interpenetrating polymer networks of polysulfone and poly acrylic acid, J. Membr. Sci. 278 (2006) 10–18.
[38] Z. Chen, M. Deng, Y. Chen, G. He, M. Wu, J. Wang, Preparation and performance of cellulose acetate/polyethyleneimine blend microfiltration membranes and their applications, J. Membr. Sci. 235 (2004) 73.
[39] B. Chakrabarty, A.K. Ghoshal, M.K. Purkait, Effect of molecular weight of PEG on membrane morphology and transport properties, J. Membr. Sci. 309 (2008) 209–221.
[40] K.F. Md Yunos, R.W. Field, Rejection amplification in the ultrafiltration of binary solute mixtures using sandwich configurations, Chem. Eng. Process. Process. Intensif. 47 (2008) 1053–1060.
[41] A.F. Ismail, P.Y. Lai, Effects of phase inversion and rheological factors on formation of defect-free and ultrathin-skinned asymmetric polysulfone membranes for gas separation, Sep. Purif. Technol. 33 (2003) 127–143.
[42] M.-J. Han, S.-T. Nam, Thermodynamic and rheological variation in polysulfone solution by PVP and its effect in the preparation of phase inversion membrane, J. Membr. Sci. 202 (2002) 55–61.
[43] G.S. Casuccio, S.F. Schlaegle, T.L. Lersch, G.P. Huffman, Y. Chen, N. Shah, Measurement of fine particulate matter using electron microscopy techniques, Fuel Process. Technol. 85 (2004) 763–779.
[44] E. Nordmeier, Advances in polyelectrolyte research: counterion binding phenomena, dynamic processes and the helix coil transition of DNA, Macromol. Chem. Phys. 196 (1995) 1321–1374.
[45] E. Tsuchida, H. Nishide, Polymer–metal complexes and their catalytic activity, Adv. Polym. Sci. 24 (1977) 1–87.
[46] W. Brian, J.J.H. Stanton, M.D. Muller, M.L. Bruening, Ultrathin multilayered polyelectrolyte films as nanofiltration membranes, Langmuir 19 (2003) 7038–7042.